Research Article

Journal of Applied Toxicology

Received: 28 May 2010, Revised: 29 July 2010, Accepted: 8 October 2010 Published online in Wiley Online Library: 8 January 2011

(wileyonlinelibrary.com) DOI 10.1002/jat.1611

Nano-CuO inhibited voltage-gated sodium current of hippocampal CA1 neurons via reactive oxygen species but independent from G-proteins pathway

Liu Zhaowei,[a] Liu Shichang,[a] Ren Guogang,[b] Zhang Tao[c] and Yang Zhuo[a]*

ABSTRACT: The aim of this study was to investigate the effects of nano-CuO on voltage-gated sodium current (I_{Na}) in hippocampal CA1 neurons. The results suggested that nano-CuO inhibited amplitudes of I_{Na} currents and prolonged peak rise time of action potential (AP). The responses to nano-CuO were inhibited by reactive oxygen species (ROS) scavenger. However, the G-proteins inhibitor did not block the effects of nano-CuO. The effects of nano-CuO were mediated through activation of ROS-I_{Na}-AP signaling cascades and independent from G-proteins pathway. Copyright © 2011 John Wiley & Sons, Ltd.

Keywords: nano-CuO; voltage-gated sodium current; hippocampus; reactive oxygen species

INTRODUCTION

Copper oxide nanoparticles (nano-CuO) potentially have wide industrial use in applications such as a heat transfer fluid in machine tools and catalytic processes (Jiang and Zhang, 2010; Song *et al*., 2010). There is increasing scientific evidence that these physical and chemical properties of manufactured nano particles lead to an increase in bioavailability and toxicity (Nel *et al*., 2006). Nano particles can cross most strong biological barriers such as the blood–brain barrier (BBB) (Lockman *et al*., 2003), which suggested that nano particles may have potential effects on neurons.

Ion channels play an important role in cell viability and function, especially in the central nervous system (CNS), and their functional properties serve as a subtle indicator of the condition and viability of the cells. Voltage-gated sodium current (I_{Na}) is responsible for modifying neuronal cellular and network excitability and activity. Therefore, potential modulation of the functional properties of I_{Na} would be expected to alter the functions of CNS neurons by nano-CuO.

However, few studies have investigated the direct effects of nano-CuO on ion channels of neuron and the potential mechanisms involved in these effects. The aim of the present study was to explore the potential neurotoxicity of nano-CuO on I_{Na} in rat hippocampal slices with whole cell patch-clamp technique.

MATERIALS AND METHODS

Slice Preparation

Male Wistar rats, bred in the Experimental Animal Center of Chinese Academy of Medical Sciences, were used on postnatal days 14–18. The experiments were conducted in accordance with the guidelines of the Medical Experimental Animal Administrative Committee of Nation. Horizontal slices that included the entire hippocampus and subiculum (400 μm in thickness) were prepared with a vibratome (VT1000M/E, Leica, Germany) and incubated with artificial cerebrospinal fluid (ACSF) containing (in mM): 125 NaCl, 25 $NaHCO_3$, 1.25 KCl, 1.25 KH_2PO_4, 1.5 $MgCl_2$, 2.0 $CaCl_2$ and 16 glucose. The standard pipette solution for recording sodium current contained (in mM): CsCl 140, $MgCl_2$ 2, Hepes 10, EGTA 10, tetraethyl ammonium chloride (TEA-Cl) 20 and Mg-ATP 2, buffered to pH 7.2 with CsOH. The standard pipette solution for current-clamp experiments was (in mM): KCl 130, $CaCl_2$ 1, $MgCl_2$ 2, EGTA 10, Hepes 10 and Mg-ATP 2, buffered to pH 7.2 with KOH. 4-Aminopyridine (4-AP) (10 mM) and $CdCl_2$ (200 μM) were added extracellularly to record I_{Na}.

Slices were maintained in ACSF for at least 1 h before moved into the recording chamber. During recordings, the slices were kept submerged in a chamber and perfused with ACSF. During the experiments, the ACSF was saturated with 95% O_2 and 5% CO_2.

*Correspondence to: Yang Zhuo, College of Medicine, Key Laboratory of Bioactive Materials, Ministry of Education, Nankai University, Tianjin 300071, China.
E-mail: zhuoyang@nankai.edu.cn

[a]College of Medicine, Key Laboratory of Bioactive Materials, Ministry of Education, Nankai University, Tianjin 300071, China

[b]Science and Technology Research Institute, University of Hertfordshire, Hatfield, Herts AL10 9AB, UK

[c]College of Life Science, Nankai University, Tianjin 300071, China

Nano-CuO Particles and Solutions

Nano particles of CuO were provided by Research Institute of Science and Technology (RSTI), University of Hertfordshire, Herts, UK. Nano particles of CuO were compounded at Queen Mary University of London using the raw materials originally obtained from QinetiQ Nanomaterials Ltd, produced through Plasma (QNL Tesima™) Technology, UK.

The characteristics of nano-CuO particles, including the size, surface area and composition of oxygen and cupper, have been described in our previously work (Xu *et al*., 2009). The particle size of nano-CuO suspension (5×10^{-5} g ml^{-1}) in ACSF was characterized by dynamic light scattering (DLS) using a Zeta-PALS + BI-90Plus (Brookhaven Instruments Corp., USA) at a wavelength of 635 nm. The scattering angle was fixed at 90°. They had a wide range from 47.94 to 311.00 nm due to the aggregation, and the hydrodynamic mean diameter was 245.9 nm in ACSF.

Stock solution (10^{-3} g ml^{-1}) of nano-CuO was prepared in Milli-Q water and dispersed by ultrasonic vibration for 20 min. Its suspension was stirred on vortex agitator before every use.

Drug Application

N-ethylmaleimide (NEM) was purchased from Alexis (USA) and *N*-(mercaptopropionyl)-glycine (*N*-MPG) was obtained from Sigma-Aldrich (USA). All drugs were prepared as stock solutions and diluted directly in ACSF to yield the appropriate concentration when used and the final DMSO (dissolved in dimethyl sulfoxide) concentration was <0.1% respectively.

Electrophysiological Recordings and Drug Application

For whole-cell recording, slices were transferred to a recording chamber (1 ml volume) placed on the stage of a modified upright infrared DIC microscope equipped with Nomarski optics. Hippocampal CA1 neurons were visualized on a television monitor connected to a low-light-sensitive CCD camera. Recordings were performed using conventional patch-clamp techniques. Signals were filtered at 3 kHz and digitized at a sampling rate of 5 kHz. The series resistance was compensated by at least 60%. Leakage and capacitive currents were subtracted on-line using a P/4 subtraction procedure.

Data acquisition was performed on computer using EPC10 patch-clamp amplifier (HEKA, Germany). After seal formation and membrane rupture, the cells were allowed to stabilize for 3–5 min before starting pulse protocols.

Tetrodotoxin (TTX)-sensitive sodium current carries the largest inward current. In whole cell patch clamp recording, cells were held at −70 mV, and current-voltage (*I–V*) curves and the steady-state activation of I_{Na} were obtained by applying depolarizing pulses from −70 to +70 mV at 10 mV steps for 20 ms. The activated inward current was completely and reversibly blocked by bath application of 0.5 μM TTX (data not shown), indicating that the voltage-gated sodium channels (VGSCs) expressed in hippocampal CA1 neurons are brain-type TTX-sensitive.

The steady-state inactivation of I_{Na} was obtained by a double-pulse protocol; a 100 ms conditioning prepulse was applied to potentials between −80 and +20 mV in 10 mV increments, followed by a 20 ms pulse to −30 mV, and holding potential at −70 mV. Peak amplitudes for I_{Na} current were normalized and plotted vs prepulse potentials.

In order to determine the kinetics of recovery from the inactivated channel state, cells were held at −70 mV, a 12 ms conditioning pulse to −30 mV was applied to inactivate the VGSCs fully and then a 60 ms test pulse to −30 mV was applied after a series of −70 mV pulses in intervals varying from 2 to 24 ms. All experiments were performed at room temperature (22–24 °C).

In the current-clamp mode, neurons were held at −70 mV, and a single action potential was elicited using a 10 ms depolarizing current pulse. Resting membrane potentials (RMPs) were recorded using current-clamp recordings.

TTX was purchased from the Research Institute of the Aquatic Products of Hebei (China). 4-AP, TEA-Cl, CsOH, CdCl, EGTA, Hepes and Mg-ATP were purchased from Sigma (St Louis, MO, USA), and other reagents were analytical research grade.

Data Analysis

All data were analyzed using Clampfit 9.0 and Origin 7.0. For activation, currents at each test potential were converted to conductance (G) using the following formula: $G = I/(V - V_k)$, where V_k is reversal potential. The peak conductance value for each test potential was normalized to G_{max} and plotted against the test potential to produce voltage–conductance relationship curves, which were fitted using Boltzmann functions $G/G_{max} = 1/\{1 + \exp[(V - V_h)/k]\}$, where V_h is the voltage at which conductance is half-maximal and k is the slope factor.

Steady-state inactivation curves were fitted with the Boltzmann equations, $I/I_{max} = 1/\{1 + \exp[(V - V_h)/k]\}$, where I/I_{max} is normalized current, V_h the potential for half-maximal inactivation and k is the slope factor. The time course of recovery of the I_{Na} currents from inactivation was fitted with a monoexponential function $I/I_{max} = A^*\{1 - \exp[-\Delta t/\tau]\}$, where I_{max} is the maximal current amplitude, I is the current after a recovery period of Δt, τ is the time constant and A is the amplitude coefficient.

Data are presented as mean ± SEM. Statistical significance was assessed using a Student's paired *t* test when there were only two groups involved. In the remaining cases the results were statistically analysed using one-way ANOVA followed Tukey's multiple comparison and $P < 0.05$ was considered significant. All data analyses were performed using the software SPSS 11.5.

RESULTS

Effects of Nano-CuO on Amplitude and *I–V* Relationships of I_{Na}

A final concentration of 5×10^{-5} g ml^{-1} nano-CuO was applied in the extracellular solution once currents were stable. In the study, data were obtained at 5 min after nano-CuO exposed to hippocampal CA1 neurons. The data in Fig. 2 showed very little change in time to peak when changing this size of the command pulse, which is a good indicator of a good quality recording. The peak amplitudes of I_{Na} were decreased significantly at different command potential from −40 to +40 mV ($n = 8$, $P < 0.05$ vs control), as shown in Fig. 2.

Nano-CuO decreased the amplitude from −3416.76 ± 263.91 to −2543.30 ± 252.41, and the observed effects on the I_{Na} were completely irreversible after washout (Fig. 1).

Effects of Nano-CuO on the Activation Kinetics of I_{Na}

The steady-state activation curves for I_{Na} under control and after exposed to nano-CuO are shown in Fig. 3. The values of V_h for

Journal of Applied Toxicology

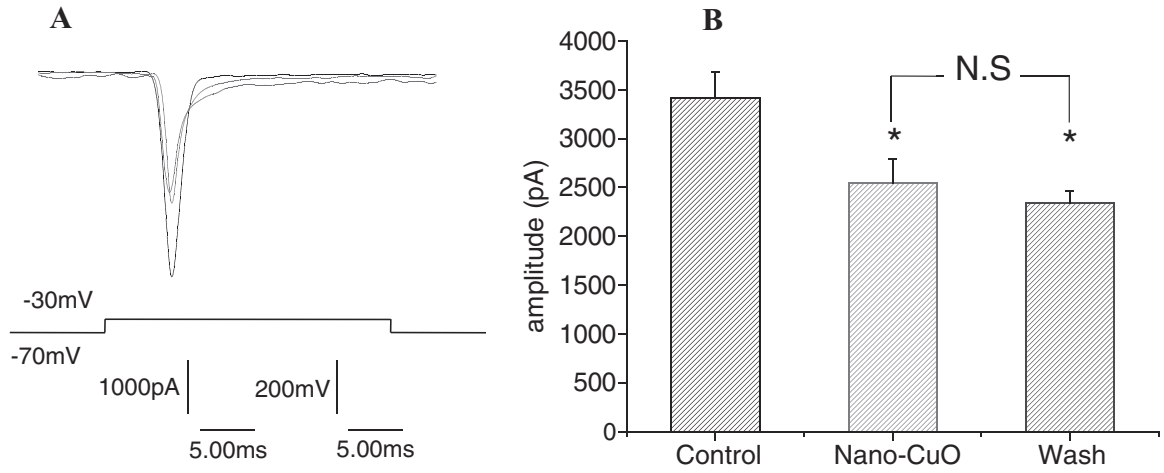

Figure 1. Effect of 5×10^{-5} g ml^{-1} nano-CuO on the amplitude of I_{Na} current. Neurons were held at –70 mV; current traces were evoked by –30 mV. (A) Averaged current traces obtained from neurons in each group. Data are presented as mean ± SEM [ANOVA, $F(2,19) = 5.698$, $P = 0.012$]. Significance levels (Turkey's test) are indicated in the figure. *$P < 0.05$ vs controls (B).

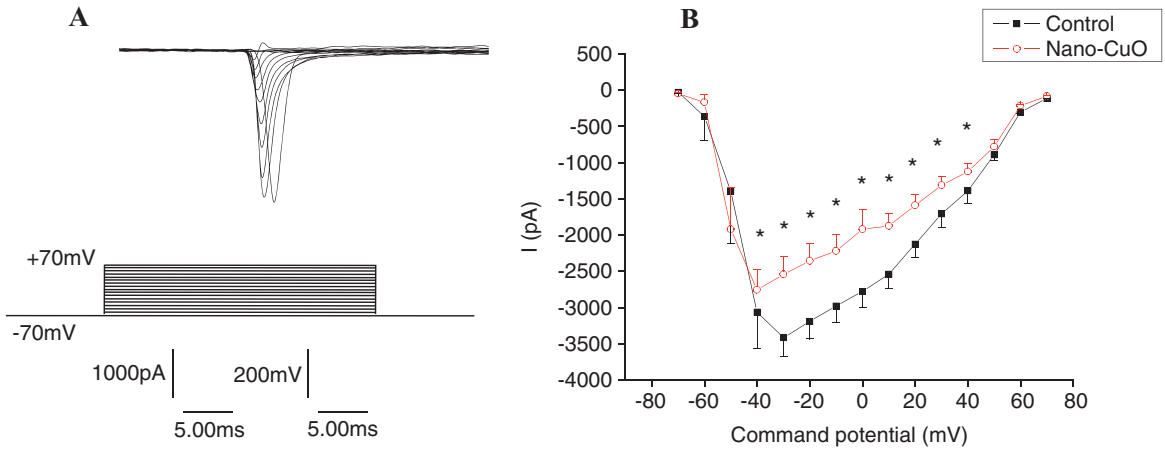

Figure 2. Effect of 5×10^{-5} g ml^{-1} nano-CuO on I_{Na}. Neurons were held at –70 mV; the current of I_{Na} was generated by applying pulses from –70 to +70 mV at 10 mV steps for 20 ms (A). The current–voltage curve of I_{Na}. (B) Each point represents mean ± SEM ($n = 8$, * $P < 0.05$ vs control).

activation of I_{Na} were –46.44 ± 2.40 mV and –54.80 ± 2.48 mV in control and nano-CuO ($n = 7$, $P < 0.05$), with a slope factor k of 0.26 ± 0.12 and 0.18 ± 0.03 ($n = 7$, $P > 0.05$), respectively. Nano-CuO produced a hyperpolarizing shift in the activation–voltage curve on I_{Na} currents with no effect on slope factor.

Effects of Nano-CuO on the Inactivation Kinetics of I_{Na}

The effects of nano-CuO on the inactivation kinetics of I_{Na} were examined (Fig. 4A). The inactivation curves were obtained through normalizing the test current amplitudes by taking the maximum value under each condition as unity (Fig. 4B). V_h for inactivation of I_{Na} were –40.15 ± 1.66 and –41.90 ± 2.24 mV in the control and nano-CuO groups ($n = 8$, $P > 0.05$ vs control), and k values were 7.73 ± 1.12 and 7.92 ± 0.49 ($n = 8$, $P > 0.05$ vs control), respectively. Nano-CuO had no effects on the inactivation–voltage curve.

Effects of Nano-CuO on the Recovery of I_{Na}

The effects of nano-CuO on the recovery time course of I_{Na} from inactivation were examined (Fig. 5A). To analyze the recovery

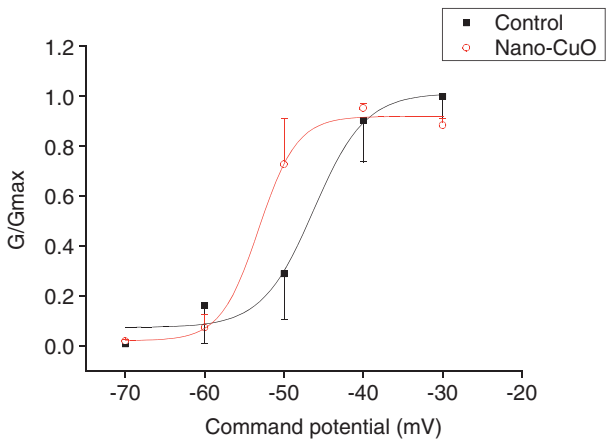

Figure 3. Effect of 5×10^{-5} g ml^{-1} nano-CuO on the steady-state activation curves of I_{Na}. Peak amplitudes of I_{Na} were converted into conductance; normalized conductance of sodium channels were plotted against the voltages of command pulses, and fitted with a Boltzmann function. Each point represents mean ± SEM ($n = 7$).

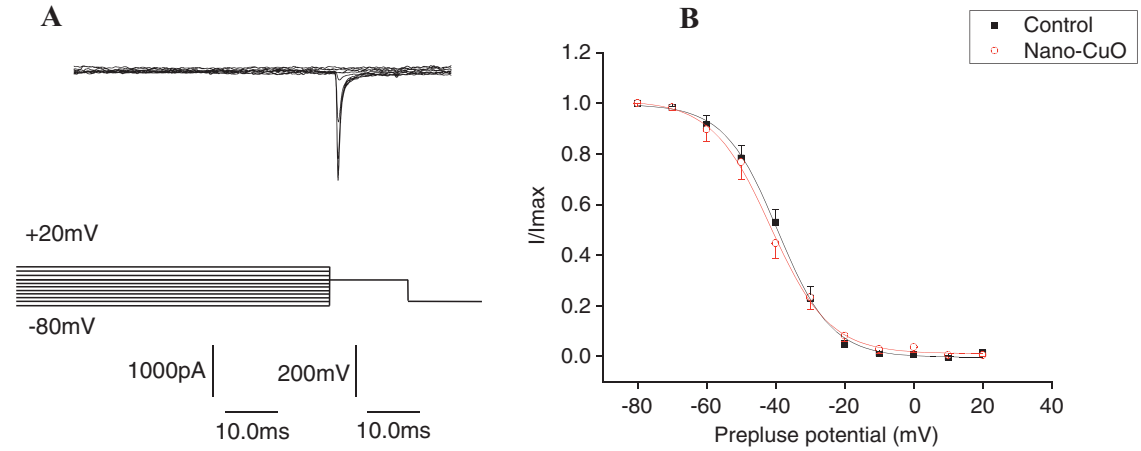

Figure 4. Effect of 5×10^{-5} g ml^{-1} nano-CuO on inactivation kinetics of I_{Na}. Currents were elicited with a 100 ms conditioning prepulse to potentials between −80 and +20 mV in 10 mV increments, followed by a 20 ms pulse of −30 mV, and holding potential at −70 mV. Peak amplitudes for I_{Na} currents were normalized and plotted vs command potentials (A), and the data were fitted with Boltzmann function (B). Each point represents mean ± SEM ($n = 8$).

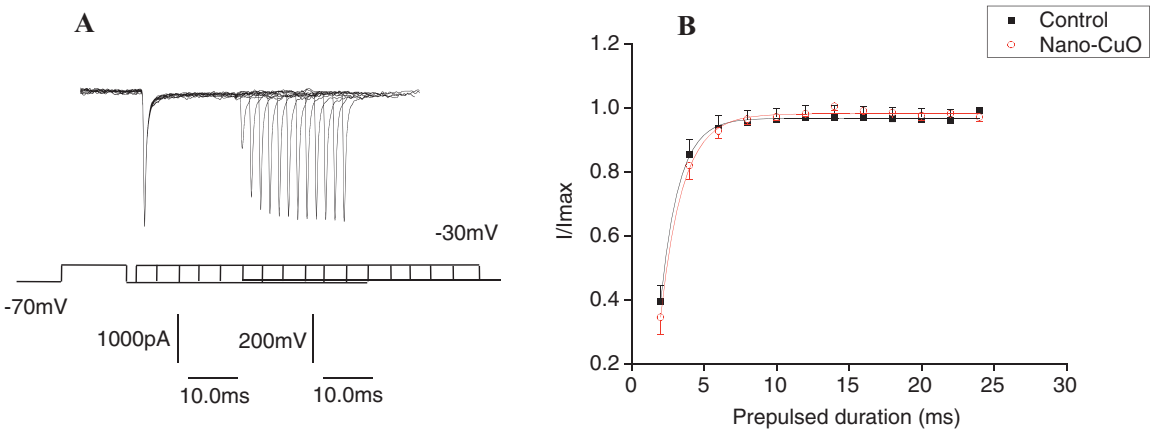

Figure 5. Effect of 5×10^{-5} g ml^{-1} nano-CuO on recovery from inactivation of I_{Na}. The currents were obtained as per the following protocol: neurons were held at −70 mV; a 12 ms conditioning depolarizing pulse to −30 mV was applied to inactivate the sodium channels fully, and then a 60 ms test pulse of −30 mV was applied after a series of −70 mV intervals varying from 2 to 24 ms. The peak value of I_{Na} evoked by the conditioning pulse was designated as I_{max}, while the peak value of I_{Na} evoked by the test pulse was designated as I. The ratio of I to I_{max} represents the recovery of I_{Na} from inactivation. (B) Each point represents mean ± SEM ($n = 8$).

time course of I_{Na}, normalized current amplitudes were plotted against the prepulse duration, and were fitted with monoexponential functions. The time constants (τ) describing the recovery time course were presented. The τ values were 1.15 ± 0.14 and 1.31 ± 0.15 ms ($n = 8$, $P > 0.05$) before and after application of nano-CuO (Fig. 5B). These results indicated that nano-CuO had no effects on the recovery of I_{Na} from inactivity.

The Inhibitory Effects by Nano-CuO were Mediated by ROS and Independent from G-proteins Pathway

Notably, nano-CuO has also been shown to exert its vasodilatory effect at least partly by the generation of reactive oxygen species (ROS; Yu *et al*., 2010). Therefore, the possibility of whether nano-CuO affected I_{Na} through a ROS-dependent mechanism was investigated. Figure 6 showed that the pretreatment of ROS scavenger *N*-MPG (300 μM) for 30 min inhibited the effects of nano-CuO on I_{Na} currents compared with that of only treatment with nano-CuO ($P < 0.05$) (Fig. 6). In order to investigate the effects of *N*-MPG (300 μM) alone on the amplitude of I_{Na}, the data were collected from neurons of pretreatment with *N*-MPG for 30 min. The results showed that *N*-MPG had no effects on I_{Na} ($P > 0.05$, Fig. 7).

According to previous reports, G-proteins were involved in the regulation of the induced changes of I_{Na} in neurons (Ma *et al*., 1994); therefore the possible contribution of G-proteins pathway in the effects of nano-CuO was examined. In the study, the G-protein inhibitor NEM (50 μM) was used. NEM had no effect on the action of nano-CuO on I_{Na} (Fig. 6).

Effects of Nano-CuO on Action Potential and RMPs

Action potential (AP) properties were examined using whole cell current-clamp recordings. Peak amplitude, spike half-width, rise

Journal of Applied Toxicology

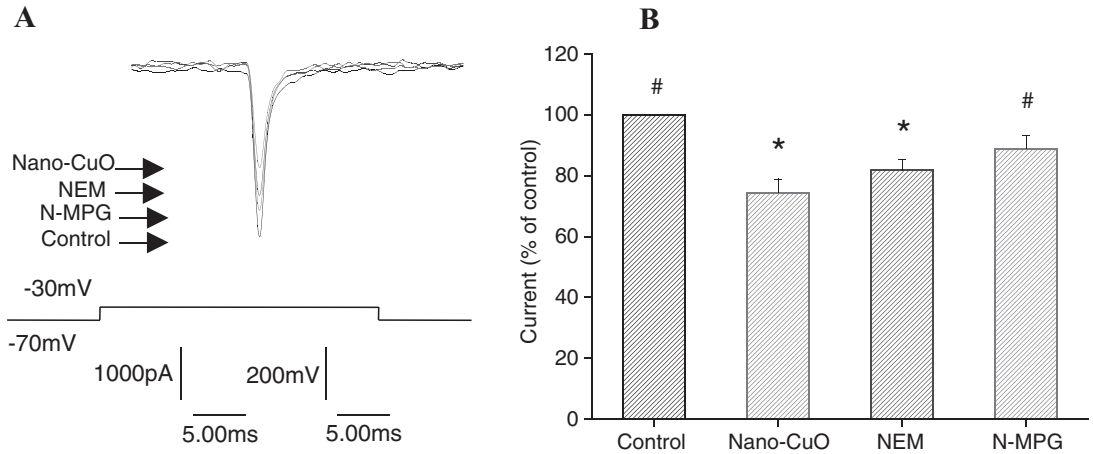

Figure 6. Neurons were held at −70 mV; current traces were evoked by −30 mV. (A) Averaged current traces obtained from neurons in each group. (B) Bar graph shows a summary of variation of I_{Na} in the presence of 5×10^{-5} g ml^{-1} nano-CuO, NEM and nano-CuO, *N*-MPG and nano-CuO. Neurons were held at −70 mV; current traces were evoked by −30 mV. Data are presented as mean ± SEM [ANOVA, $F(3, 28) = 9.214$, $P < 0.001$]. Significance levels (Turkey's test) are indicated in the figure: $^{*}P < 0.05$ vs controls; $^{\#}P < 0.05$ vs Nano-CuO.

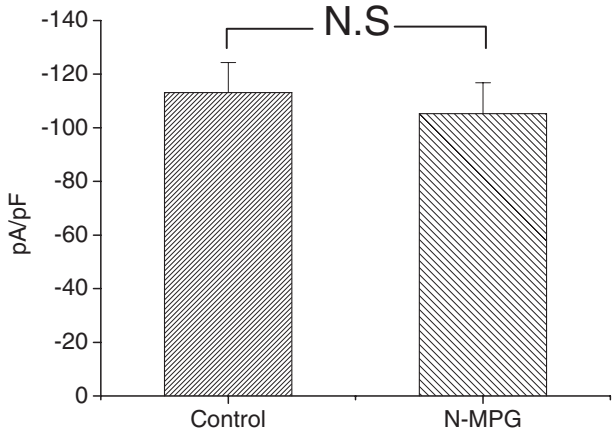

Figure 7. The effects of pretreatment with *N*-MPG (300 μM) for 30 min. N.S., not significant ($n = 9$).

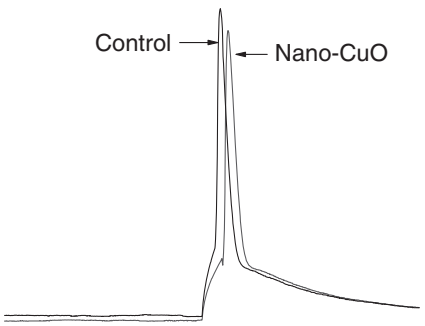

Figure 8. Effect of 5×10^{-5} g ml^{-1} nano-CuO on action potential. In the current-clamp mode, neurons were held at −70 mV, and single action potentials were elicited using a 10 ms depolarizing current pulse before and after application of nano-CuO.

time and decay time of single action potential were measured before and after drug applications for 5 min. It was found that peak amplitude was decreased; meanwhile, peak rise time was increased in the presence of the 5×10^{-5} g ml^{-1} nano-CuO solution ($n = 4$, $P < 0.05$, as shown in Fig. 8 and Table 1). RMPs became more depolarized by ~10 mV treatment with nano-CuO ($n = 7$, $P < 0.05$, as shown in Table 1).

Table 1. Effects of nano-CuO treatment for 5 min on properties of single action potential and resting membrane potential

	Control	Nano-CuO
Peak amplitude (mV)	102.24 ± 28.51	99.27 ± 3.86*
Spike half-width (ms)	2.74 ± 0.06	3.11 ± 0.37
Peak rise time (10–90%) (ms)	2.41 ± 0.06	3.62 ± 0.54*
Peak decay time (10–90%) (ms)	1.65 ± 0.06	1.63 ± 0.08
Resting membrane potential (mV)	−60.14 ± 1.34	−49.86 ± 1.78*

Action potential (AP) half-width, width of AP at point mid-way between after hyperpolarizations and peak of AP. Peak rise time, time-to-peak from 10 to 90% of amplitude, Peak decay time, time-to-after hyperpolarizations from 90 to 10% of amplitude. Values are mean ± SEM. *P*-values were obtained using two-tailed paired *t*-test ($n = 7$ in resting membrane potential, $n = 4$ else; $^{*}P < 0.05$ vs control).

DISCUSSION

Nanotechnology is a rapidly expanding and advancing field of research that has already yielded a variety of commercially available products. Since nanoparticles are more often used today in different products, there is an increased risk of exposure of workers as well as consumers and the general public. For metal oxide nanoparticles, their small size and large specific surface area endow them with high chemical reactivity and intrinsic toxicity. According to Karlsson, nano-CuO are highly toxic when compared with other metal oxide nanoparticles as well as carbon nanoparticles and carbon nanotubes (Karlsson *et al*., 2008).

Small particles have better mobility than larger ones. It is expected that transportation of nanoparticles across the BBB is possible by trans-synaptic transport (Oberdorster *et al*., 2004), carrier-mediated endocytosis (Hoet *et al*., 2004) or passive diffusion. So it is valuable to investigate the effects of nano-CuO on neurons.

VGSCs play a critical role in the generation and propagation of AP in excitable cells. In addition, VGSCs in nerve terminals can potentially influence neurotransmitter release from presynaptic nerve endings (Abita *et al*., 1977; Krueger *et al*., 1980). These integrative functions of VGSCs are likely to be subject to neuromodulation. Damage in VGSCs has been associated with a number of neurological diseases including spontaneous epilepsy and pain conditions, and have been implicated in various psychiatric disorders (Guo *et al*., 2008; Meisler and Kearney, 2005).

Impairments of functions of I_{Na} by nanoparticles during treatment have been observed in several studies *in vitro*. Tang *et al*. found nano-sized quantum dots impaired I_{Na} current in primary cultured hippocampal neuron (Tang *et al*., 2008). Our previous studies showed that nano-Ag inhibited I_{Na} in the concentration of 10^{-5} g ml^{-1} (Liu *et al*., 2009), while nano-ZnO (10^{-4} g ml^{-1}) increased the amplitudes of I_{Na} (Zhao *et al*., 2009).

According to our previous studies, the concentration of 10^{-5} g ml^{-1} might be the minimum concentration for action of nano-Ag on I_{Na} of hippocampal CA1 neurons (Liu *et al*., 2009). Since research has suggested nano-Ag is more toxic than nano-CuO (Ivask *et al*., 2010; Kahru and Dubourguier, 2010), the concentration of 5×10^{-5} was employed in the study. We reported that nano-CuO in the concentration of 5×10^{-5} inhibited delayed rectifier potassium current (I_K) and produced a negative shift on the inactivation curve of I_K (Xu *et al*., 2009).

In this study, the results showed nano-CuO inhibited the peak amplitude I_{Na}, which might result in decreases in intracellular Na^+ concentration due to decreased Na^+ influx. These may retard the exchanges of Na^+ for Ca^{2+} by Na^+–Ca^{2+} exchangers (Xiao *et al*., 2002). Since the exchanger was shown to generate inward current during the repolarization phase of the action potential (Janvier and Boyett, 1996; Janvier *et al*., 1997), the effect of I_{Na} could contribute to the change AP shape by nano-CuO. It is well established that VGSC play a role in neurotransmitter release (Sitte *et al*., 2004). Thus the effects of nano-CuO on I_{Na} also mean that modulation may be able to produce functional effects at message transmission in CNS.

It has been shown that nano-CuO produced a hyperpolarizing shift in the activation curve. The S4 segment in a subunit of VGSCs contains four to eight positively charged residues at three residue intervals. They serve as voltage sensors and initiate the voltage-dependent activation of VGSCs by moving outward under the influence of the electric field (Armstrong, 1981; Yang *et al*., 1996). Our results suggested an action on S4 segment of activation gating, resulting in conformational changes of the channel.

Although the treatment of nano-CuO altered a number of characteristics of VGSCs, this treatment was also fairly selective. For example, the steady-state inactivation, and the recovery from inactivation were almost exactly the same in both the experimental and the control neurons.

AP properties were examined for further detecting the effects of nano-CuO. Our results showed the peak amplitude of the evoked single action potential was significantly reduced; meanwhile the peak rise time was increased. According to previous reports, VGSC mediated the very rapid rising phase and was the initial component of the falling phase of AP in the excitable cells, and then was responsible for the amplitude of AP (Balser, 2001; Koopmann *et al*., 2006). These suggested that the effects of nano-CuO on AP may, at least in part, be due to the I_{Na} inhibition. According to Xie *et al*. (2007), the I_{Na} inhibitor TTX negatively shifted RMP by ~10 mV. However, nano-CuO depolarized RMP in our study with the inhibitory effects of I_{Na}. Therefore, we speculated that there might be other action sites of nano-CuO on the membrane, such as Na^+/K^+-ATPase, which plays an important role in ionic homeostasis due to ATP-dependent transport of Na^+ and K^+ (Molnar *et al*., 1999).

One main mechanism behind the health effects induced by manufactured nanoparticles is the ability to cause oxidative stress (Li *et al*., 2003; Nel *et al*., 2006; Xia *et al*., 2006). Oxidative stress occurs when ROS disturb the balance between oxidative pressure and antioxidant defense. ROS can modify proteins, lipids and DNA in the cell, which suggests that ROS might cause damage in the function of the ion channel. The brain is especially vulnerable to oxidative stress; therefore the induction of ROS might be responsible for this inhibition of I_{Na} current. According to a recent study, exposure to nano-CuO caused ROS generation in mouse pulmonary microvascular endothelial cells (Yu *et al*., 2010). Interestingly, in our study pretreatment of *N*-MPG (ROS scavenger) could inhibit the effects of nano-CuO on I_{Na} amplitude. Although the neurological toxicity of nano-CuO on I_{Na} is not clinically ascertained, several lines of evidence argue for oxidative modification of VGSC with pathophysiological consequences (Desaphy *et al*., 1998).

VGSCs can also be modulated by second messengers, including protein kinases and G-proteins (Catterall, 1993; Li *et al*., 1993; Ma *et al*., 1994). In our study, G-protein inhibitor NEM had no effects on the action of nano-CuO. The above findings supported the idea that nano-CuO inhibited I_{Na} via ROS pathway as well as G-protein-independent mechanisms.

In summary, our results show that nano-CuO inhibited the I_{Na}, and the impairment of AP properties associated with nano-CuO exposure. Our findings also confirm that the effects of nano-CuO on hippocampal neurons were mediated through activation of ROS-I_{Na}-AP signaling cascades and independent from G-proteins pathway. These results provided primary mechanisms underlying nano-CuO induced I_{Na} amplitude inhibition and added new knowledge to so-far-poor understanding of nano-CuO toxicology.

Acknowledgments

This work was partly supported by grants from the National Natural Science Foundation of China (31070890 and 31000509) and UK Royal Academy of Engineering on Major Research Exchanges Award (5502).

REFERENCES

Abita JP, Chicheportiche R, Schweitz H, Lazdunski M. 1977. Effects of neurotoxins (veratridine, sea anemone toxin, tetrodotoxin) on transmitter accumulation and release by nerve terminals *in vitro*. *Biochemistry* **16**: 1838–1844.

Armstrong CM. 1981. Sodium channels and gating currents. *Physiol. Rev.* **61**: 644–683.

Balser JR. 2001. Inherited sodium channelopathies: novel therapeutic and proarrhythmic molecular mechanisms. *Physiol. Rev.* **11**: 229–237.

Catterall WA. 1993. Structure and modulation of Na^+ and Ca^{2+} channels. *Ann. NY Acad. Sci.* **707**: 1–19.

Desaphy JF, De Luca A, Imbrici P, Conte Camerino D. 1998. Modification by ageing of the tetrodotoxin-sensitive sodium channels in rat skeletal muscle fibres. *Biochim. Biophys. Acta* **1373**: 37–46.

Guo F, Yu N, Cai JQ, Quinn T, Zong ZH, Zeng YJ, Hao LY. 2008. Voltage-gated sodium channel Nav1.1, Nav1.3 and beta1 subunit were up-regulated in the hippocampus of spontaneously epileptic rat. *Brain Res. Bull.* **75**: 179–187.

Hoet PH, Bruske-Hohlfeld I, Salata OV. 2004. Nanoparticles – known and unknown health risks. *J. Nanobiotechnol.* **2**: 12.

Ivask A, Bondarenko O, Jepihhina N, Kahru A. 2010. Profiling of the reactive oxygen species-related ecotoxicity of CuO, ZnO, TiO(2), silver and fullerene nanoparticles using a set of recombinant luminescent *Escherichia coli* strains: differentiating the impact of particles and solubilised metals. *Anal. Bioanal. Chem.* **398**: 701–716.

Janvier NC, Boyett MR. 1996. The role of Na–Ca exchange current in the cardiac action potential. *Cardiovasc. Res.* **32**: 69–84.

Janvier NC, McMorn SO, Harrison SM, Taggart P, Boyett MR. 1997. The role of Na(+)–Ca^{2+} exchange current in electrical restitution in ferret ventricular cells. *J. Physiol.* **504**(Pt 2): 301–314.

Jiang LC, Zhang WD. 2010. A highly sensitive nonenzymatic glucose sensor based on CuO nanoparticles-modified carbon nanotube electrode. *Biosens. Bioelectron.* **25**: 1402–1407.

Kahru A, Dubourguier HC. 2010. From ecotoxicology to nanoecotoxicology. *Toxicology* **269**: 105–119.

Karlsson HL, Cronholm P, Gustafsson J, Moller L. 2008. Copper oxide nanoparticles are highly toxic: a comparison between metal oxide nanoparticles and carbon nanotubes. *Chem. Res. Toxicol.* **21**: 1726–1732.

Koopmann TT, Bezzina CR, Wilde AA. 2006. Voltage-gated sodium channels: action players with many faces. *Ann. Med.* **38**: 472–482.

Krueger BK, Blaustein MP, Ratzlaff RW. 1980. Sodium channels in presynaptic nerve terminals. Regulation by neurotoxins. *J. Gen. Physiol.* **76**: 287–313.

Li M, West JW, Numann R, Murphy BJ, Scheuer T, Catterall WA. 1993. Convergent regulation of sodium channels by protein kinase C and cAMP-dependent protein kinase. *Science* **261**: 1439–1442.

Li N, Hao M, Phalen RF, Hinds WC, Nel AE. 2003. Particulate air pollutants and asthma. A paradigm for the role of oxidative stress in PM-induced adverse health effects. *Clin. Immunol.* **109**: 250–265.

Liu Z, Ren G, Zhang T, Yang Z. 2009. Action potential changes associated with the inhibitory effects on voltage-gated sodium current of hippocampal CA1 neurons by silver nanoparticles. *Toxicology* **264**: 179–184.

Lockman PR, Oyewumi MO, Koziara JM, Roder KE, Mumper RJ, Allen DD. 2003. Brain uptake of thiamine-coated nanoparticles. *J. Control Release* **93**: 271–282.

Ma JY, Li M, Catterall WA, Scheuer T. 1994. Modulation of brain Na^+ channels by a G-protein-coupled pathway. *Proc. Natl Acad. Sci. USA* **91**: 12351–1235.

Meisler MH, Kearney JA. 2005. Sodium channel mutations in epilepsy and other neurological disorders. *J. Clin. Invest.* **115**: 2010–2017.

Molnar LR, Thayne KA, Fleming WW, Taylor DA. 1999. The role of the sodium pump in the developmental regulation of membrane electrical properties of cerebellar Purkinje neurons of the rat. *Brain Res. Dev. Brain Res.* **112**: 287–91.

Nel A, Xia T, Madler L, Li N. 2006. Toxic potential of materials at the nanolevel. *Science* **311**: 622–627.

Oberdorster G, Sharp Z, Atudorei V, Elder A, Gelein R, Kreyling W, Cox C. 2004. Translocation of inhaled ultrafine particles to the brain. *Inhal. Toxicol.* **16**: 437–445.

Sitte HH, Farhan H, Javitch JA. 2004. Sodium-dependent neurotransmitter transporters: oligomerization as a determinant of transporter function and trafficking. *Mol. Interv.* **4**: 38–47.

Song MJ, Hwang SW, Whang D. 2010. Non-enzymatic electrochemical CuO nanoflowers sensor for hydrogen peroxide detection. *Talanta* **80**: 1648–1652.

Tang M, Xing T, Zeng J, Wang H, Li C, Yin S, Yan D, Deng H, Liu J, Wang M, Chen J, Ruan DY. 2008. Unmodified CdSe quantum dots induce elevation of cytoplasmic calcium levels and impairment of functional properties of sodium channels in rat primary cultured hippocampal neurons. *Environ. Health Perspect.* **116**: 915–922.

Xia T, Kovochich M, Brant J, Hotze M, Sempf J, Oberley T, Sioutas C, Yeh JI, Wiesner MR, Nel AE. 2006. Comparison of the abilities of ambient and manufactured nanoparticles to induce cellular toxicity according to an oxidative stress paradigm. *Nano Lett.* **6**: 1794–1807.

Xiao AY, Wei L, Xia S, Rothman S, Yu SP. 2002. Ionic mechanism of ouabain-induced concurrent apoptosis and necrosis in individual cultured cortical neurons. *J. Neurosci.* **22**: 1350–1362.

Xie M, Lynch DT, Schools GP, Feustel PJ, Kimelberg HK, Zhou M. 2007. Sodium channel currents in rat hippocampal NG2 glia: characterization and contribution to resting membrane potential. *Neuroscience* **150**: 853–862.

Xu LJ, Zhao JX, Zhang T, Ren GG, Yang Z. 2009. *In vitro* study on influence of nano particles of CuO on CA1 pyramidal neurons of rat hippocampus potassium currents. *Environ. Toxicol.* **24**: 211–217.

Yang N, George AL Jr, Horn R. 1996. Molecular basis of charge movement in voltage-gated sodium channels. *Neuron* **16**: 113–122.

Yu M, Mo Y, Wan R, Chien S, Zhang X, Zhang Q. 2010. Regulation of plasminogen activator inhibitor-1 expression in endothelial cells with exposure to metal nanoparticles. *Toxicol. Lett.* **195**: 82–89.

Zhao J, Xu L, Zhang T, Ren G, Yang Z. 2009. Influences of nanoparticle zinc oxide on acutely isolated rat hippocampal CA3 pyramidal neurons. *Neurotoxicology* **30**: 220–230.